3D imaging of magnetic particles using the 7-channel magnetoencephalography device without pre-magnetization or displacement of the sample

M.A. Polikarpov[a,*], M.N. Ustinin[b], S.D. Rykunov[b], A.Y. Yurenya[a,c], S.P. Naurzakov[a], A.P. Grebenkin[a], V.Y. Panchenko[a,c]

[a] National Research Center "Kurchatov Institute", Moscow, Russia
[b] Institute of Mathematical Problems of Biology, Russian Academy of Sciences, Pushchino, Russia
[c] Faculty of Physics, Lomonosov Moscow State University, Moscow, Russia

ARTICLE INFO

ABSTRACT

SQUID-based magnetoencephalography device was used for the measurement of a magnetic noise generated by ferrofluid in the stationary standing vial. It was found that a free surface of the ferrofluid generates spontaneous magnetic field sufficient to detect the presence of nanoparticles in the experimental setup. The spatial distribution of elementary magnetic sources was reconstructed by the frequency-pattern analysis of multi-channel time series. The localization of ferrofluids was performed based on the analysis of quasirandom time series in two cases of oscillation source. One of them was infrasound from outer noise, and another one was the human heartbeat. These results are prospective for 3D imaging of magnetic particles without pre-magnetization.

1. Introduction

The transparency of biological tissue to low-frequency magnetic fields permits the magnetic particles imaging (MPI) within the body. Usually the MPI method requires a sample containing the superparamagnetic particles, an oscillating magnetic field and/or a static magnetic field, and a magnetic field detector, which can be based on receive coils [1] or superconducting quantum interference devices (SQUID) [2]. The high sensitivity of SQUIDs allows the detection of magnetic nanoparticles in the samples subjected to the motion in the geomagnetic field instead of the pre-magnetization [3]. The possibility of the detection of magnetic nanoparticles in the ferrofluid using 151-channel SQUIDs based magneto-encephalography (MEG) device without pre-magnetization and mechanical movement of the sample was first demonstrated in [4]. The authors of the last paper installed a glass vial of magnetite nanoparticles based ferrofluid at stationary location within the MEG helmet region. They found that the frequency spectrum of the MEG data with the sample present was greater than the baseline sensor noise. Furthermore, the comparison between spatial contour maps of the frequency data measured without the sample and with the sample showed a distinct increase in frequency power just at the location of the sample. These results pointed to the possibility of MEG imaging of magnetic nanoparticles within living organisms.

The purposes of our work were to clarify the physical mechanism of the magnetic signal generation by the stationary vial of ferrofluid inside the MEG device and to verify the possibility of using the effect for the 3D imaging of ferrofluids.

2. Materials and methods

2.1. Synthesis of ferrofluids

Magnetite nanoparticles were prepared by sol-gel method. Aqueous solutions of iron chloride (1 g. $FeCl_2 \times 4H_2O$ + 2,72 g. $FeCl_3 \times 6H_2O$) were added to the 125 ml of 0.7 M ammonia solution and stirred vigorously for 30 min. Then the resulting suspension was precipitated on the magnet and the supernatant was poured. Then, the resulting precipitate was washed 4 times with aqueous solution of citrate (20 mg/ml), each time the suspension was precipitated on a magnet and the supernatant was poured. Water was then added to the precipitate. The mean size of the resulting nanoparticles 10–12 nm was evaluated by the Mossbauer spectroscopy method.

---

* Corresponding author.
E-mail address: polikarpov_imp@mail.ru (M.A. Polikarpov).
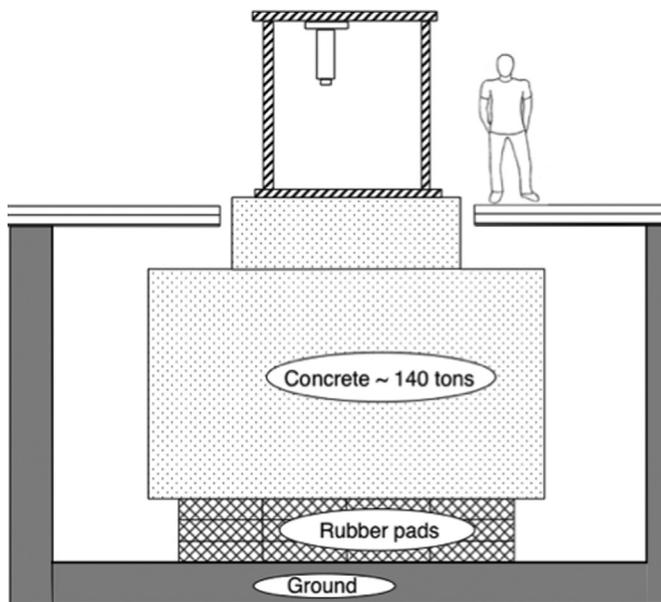
Fig. 1. The structure of the vibration-isolated foundation under the camera with the 7-channel MEG device situated in National Research Center "Kurchatov institute", Moscow.

2.2. Multichannel magnetic measurements

The measurements were carried out at 7-channel MEG device, designed for non-contact recording of a magnetic encephalogram of a human brain [5,6]. The planar set of sensors has a hexagonal structure and includes 7 second-order SQUID gradiometers. One gradiometer is located in the center of the hexagon. The distances between the gradiometers are 30 mm. The sensors demonstrate an intrinsic noise level lower than 5 fT/√Hz.

The MEG device is placed inside a thick-walled aluminum camera, designed for shielding from an alternating electromagnetic field. No shielding from static magnetic field is used. The camera is placed on the vibration-isolated foundation, shown in the Fig. 1. The total noise level of about 20–40 fT/√Hz was measured at urban conditions of Moscow city.

2.3. Data analysis

Quasirandom time series were recorded by the MEG device and then processed with recently developed method [7–9], based on the Fourier transform and coherence analysis. The method was developed in [7] to study various complex systems, and was applied to investigate the human brain spontaneous activity [8–10].

At the first step of this method, the set of discrete experimental vectors $\{\mathbf{b}_k\}$ is transformed into the set of continuous functions $\{\widetilde{B}_k(t)\}$:

$$\widetilde{B}_k(t)=F(\mathbf{b}_k,\ t),\ t\in[0,T],\ k=1,\ldots,K. \tag{1}$$

where T is the time of measurement, k is the channel number, F is a function corresponding to the particular interpolation methodology [11]. The multichannel Fourier transform calculates a set of spectra for interpolated experimental functions:

$$a_{nk}=\frac{2}{T}\int_0^T \widetilde{B}_k(t)\cos(2\pi\nu_n t)dt,\ b_{nk}=\frac{2}{T}\int_0^T \widetilde{B}_k(t)\sin(2\pi\nu_n t)dt, \tag{2}$$

where a_{nk}, b_{nk} are Fourier coefficients for the frequency ν_n in the channel number k, and $n=1,\ldots N$, $N=\nu_{max}T$, where ν_{max} is the highest desirable frequency. The coefficient for $n=0$ is not considered, because the constant field component has no meaning in SQUID measurements.

To reveal the detailed frequency structure of the system, all spectra are calculated for the whole time of registration. The step in frequency is equal to $\Delta\nu=\nu_n-\nu_{n-1}=1/T$, thus frequency resolution is determined by the recording time. Gaussian quadrature formulas are used to calculate integrals for any interval [0, T]. In this study, all time series were measured for 20 min, thus providing frequency resolution 0,000833 Hz. In order to study the system in frequency space, we restore multichannel signal at every frequency ν_n in all channels and analyze the functions obtained:

$$B_{nk}(t)=\rho_{nk}\sin(2\pi\nu_n t+\varphi_{nk}), \tag{3}$$

where $\rho_{nk}=\sqrt{a_{nk}^2+b_{nk}^2}$, $\varphi_{nk}=$atan2$(a_{nk},\ b_{nk})$, a_{nk}, b_{nk} are Fourier coefficients, found in (2), $t\in[0,T_{\nu_n}]$, $T_{\nu_n}=1/\nu_n$ is the period of this frequency.

If $\varphi_{nk}=\varphi_n$, then formula (3) describes a coherent multichannel oscillation and can be written as

$$B_{nk}(t)=\rho_n\hat{\rho}_{nk}\sin(2\pi\nu_n t+\varphi_n), \tag{4}$$

where $\rho_n=\sqrt{\sum_{k=1}^K\rho_{nk}^2}$ is the amplitude, and $\hat{\rho}_{nk}=\rho_{nk}/\rho_n$ is the normalized pattern of oscillation. The normalized pattern $\hat{\rho}_{nk}$ makes it possible to determine the spatial structure of the source from the inverse problem solution, and this structure is constant throughout the entire period of the oscillation. The time course of the field is determined by the function $\rho_n\sin(2\pi\nu_n t+\varphi_n)$ which is common for all channels, i.e. this source is oscillating as a whole at the frequency ν_n.

The theoretical foundations for the reconstruction of static functional entities, or sources, have been developed in [7–9]. This reconstruction is based on detailed frequency analysis and extraction of the frequencies, having high coherence and similar patterns.

The algorithm of massive frequency-pattern analysis was formulated as:

1. Fourier Transform of the multichannel signal.
2. Inverse Fourier Transform – restoration of the signal at each frequency.
3. If the coherence at the particular frequency is close to 1, then use the pattern and frequency as elementary coherent oscillation.
4. If the restored signal consists of several phase-shifted coherent oscillations, then extract those oscillations.

After the fourth step of this analysis, the initial multichannel signal is represented as a sum of elementary coherent oscillations:

$$B_k(t)\cong\sum_{n=1}^N\sum_{m=1}^M D_{mn}\hat{\rho}_{mnk}\sin(2\pi\nu_n t+\varphi_{mn}),\nu_n=n/T,\ N=\nu_{max}T, \tag{5}$$

where M is maximal number of coherent oscillations, extracted at the frequency ν_n.

Each elementary oscillation is characterized by frequency ν_n, phase φ_{mn}, amplitude D_{mn}, normalized pattern $\hat{\rho}_{mn}$ and is produced by the functional entity having a constant spatial structure.

The method of functional tomography reconstructs the structure of the system from the analysis of the set of normalized patterns $\{\hat{\rho}_{mn}\}$. The functional tomogram displays a 3-dimensional map of the energy produced by all the sources located at a given point. In order to build a functional tomogram, the space under study is divided into $N_x\times N_y\times N_z$ elementary cubicles with centers in $\mathbf{r}_{ijs}$. The edge of the cubicle (spatial resolution) in this study is 1 mm. To calculate the energy produced by all the sources located in the center of the cubicle, the set of L trial magnetic dipoles $\mathbf{Q}_{ijsl}$ is build. The magnetic induction from the trial source can be derived from [12] for the coil with current I, radius a and direction $\mathbf{Q}_{ijsl}$, located in $\mathbf{r}_{ijs}$. For the sensor with location $\mathbf{r}_k$ and direction $\mathbf{n}_k$, the element of the trial pattern will be:

$$\rho_{ijslk}^{tr} = \frac{\mu_0 I}{\pi \alpha^2 \beta}\left(\left(\frac{z}{d}(\alpha^2(E(\gamma^2) - K(\gamma^2)) - 2adE(\gamma^2))\boldsymbol{e_d} + \right.\right.$$

$$\left.\left. (\alpha^2(K(\gamma^2) - E(\gamma^2)) + +(2a^2 + 2ad)E(\gamma^2))\boldsymbol{Q_{ijsl}}\right), \ \boldsymbol{n_k}\right), \qquad (6)$$

where $\alpha^2 = a^2 + d^2 + z^2 - 2da$; $\beta^2 = a^2 + d^2 + z^2 + 2da$; $\gamma^2 = 1 - \frac{\alpha^2}{\beta^2}$;

$\boldsymbol{r_a} = \boldsymbol{r_k} - \boldsymbol{r_{ijs}}$; $z = (\boldsymbol{r_a}, \ \boldsymbol{Q_{ijsl}})$; $\boldsymbol{d} = \boldsymbol{r_a} - z\boldsymbol{Q_{ijsl}}$; $d = |\vec{d}|$; $\boldsymbol{e_d} = \frac{\boldsymbol{d}}{|d|}$; $|\boldsymbol{n_k}| = 1$;

$K(\gamma^2)$ - elliptic integral of the first kind, $E(\gamma^2)$ - elliptic integral of the second kind.

Trial dipoles uniformly cover the sphere in L directions, in this study $L = 62$. Then the set of normalized trial patterns is calculated:

$$\hat{\boldsymbol{\rho}}_{ijsl}^{tr}, \ i = 1, ..., N_x; j = 1, ..., N_y; s = 1, ..., N_z; l = 1, ..., L. \qquad (7)$$

In this study, 62 millions of trial patterns are used for the functional tomography of the experimental space $100 \times 100 \times 100$ cubic millimeters.

For each normalized experimental pattern in (5), $\hat{\boldsymbol{\rho}}_{mn}$, the following function is calculated, giving the difference between this pattern and one of the trial patterns:

$$\chi(i, \ j, \ s, \ l) = \sum_{k=1}^{K}(\hat{\rho}_{mnk} - \hat{\rho}_{ijslk}^{tr})^2. \qquad (8)$$

The position and direction of the source producing the pattern $\hat{\boldsymbol{\rho}}_{mn}$ are determined by numbers (I, J, S, L) providing the minimum to the function $\chi(i, j, s, l)$ over the variables

$i = 1, ..., N_x; j = 1, ..., N_y; s = 1, ..., N_z; l = 1, ..., L.$

The energy of this source D_{mn}^2 is added to the energy produced from the cubicle with the center at $\boldsymbol{r}_{IJS}$.

Performing this procedure for all normalized experimental patterns: $m = 1, ..., M$; $n = 1, ..., N$, it is possible to distribute in space the energy of all oscillations from formula (5). The result of such distribution is the functional tomogram of the experimental space, reconstructed from multichannel magnetic recordings.

In order to estimate general spectral features of various experimental data, we use the sum of powers in all channels:

$$\text{Power}(\nu_n) = \sum_{k=1}^{K} \rho_{nk}^2, \qquad (9)$$

where ρ_{nk} is calculated in (3).

3. Results and discussion

3.1. Study of the dependence of the noise spectrum from the position of the vial with ferrofluid

The synthesized ferrofluid was placed in a 40 ml plastic vial. The vial was placed on a nonmagnetic stand situated at 8 cm under the measuring head of the MEG device. 7 numerated circular areas were marked on the surface of the stand. Each circle was located just under the center of corresponding SQUID gradiometer (see inset at Fig. 2). MEG noise recordings were collected with the sample in the positions 1 and 6 and without the sample. The duration of one recording was 20 min. Fourier transform of the signals from each SQUID channel was generated. Then the summary power in all channels was calculated (9). The change of the spectrum of the noise generated by the vial with ferrofluid after replacing the vial from the position under channel 1 to the position under channel 6 is shown in the Fig. 2. It was found that the transfer of the vial with ferrofluid to the distance of 3 cm changes the amplitude of the noise spectrum in the frequency band 5–6 Hz. It should be mentioned that the vial with ferrofluid does not generate its own new spectral component of the noise, more or less enhancing the
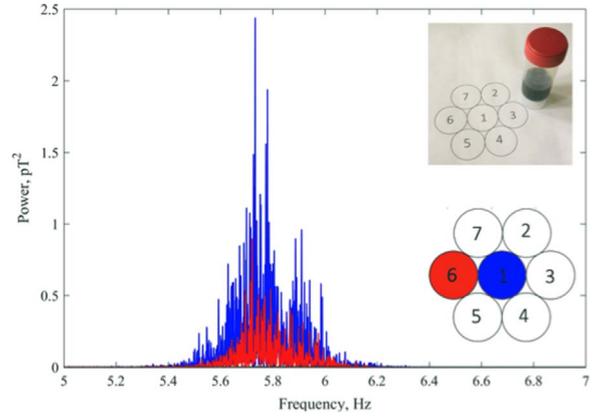
Fig. 2. The spectra of the noise generated by the vial with the ferrofluid, situated under channel 1 (blue) and channel 6 (red) of the MEG device. Black – the spectrum of the noise without vial, less than 1% of maximal power. (For interpretation of the references to color in this figure legend, the reader is referred to the web version of this article.)

inherent noise of the experimental setup.

3.2. Identification of the source of the noise generated by the vial with ferrofluid in the MEG device

Faraday's law of induction states that the induced electromotive force in any closed circuit (in SQUID in our case) is equal to the negative of the time rate of change of the magnetic flux enclosed by the circuit. Accordingly the observed phenomenon can be explained in the framework of the next model. Magnetization vectors of superparamagnetic nanoparticles are oriented by the Earth's magnetic field. Oriented magnetic particles move and generate alternating field, which generates current in the antennas of the gradiometers. So, the task of an identification of the source of the magnetic noise reduces to the identification of the source of the movement of nanoparticles in the "motionless" vial. The authors of [4] suggested that the change of the magnetic flux from the stationary standing glass with ferrofluid could be caused by both the random fluctuations of the magnetic moments of magnetic nanoparticles due to Neel relaxation and the Brownian rotation/movement of the particles in a colloidal liquid. On the other hand the frequency range of the fluctuations < 7 Hz (see Fig. 2) looks too low for the Neel process. The Neel relaxation frequency for similar magnetite single-domain nanoparticles was many times evaluated from Mossbauer measurements and proved to be about 100 MHz.

It is known that the mechanical oscillations of SQUID magnetometer in the geomagnetic field can strongly influence its reading [13]. Even a tree swing in the wind can generate an appreciable spurious signal in the SQUID magnetometer, standing at a considerable distance [14]. Therefore in this study we examined three possible sources of the movement.

- Brownian motion of the particles in the ferrofluid.
- Vibrations of the vial with ferrofluid as a whole.
- Fluctuations on the free surface of the ferrofluid (Faraday waves).

In order to clarify the physical mechanism of the magnetic signal generation we have studied the changes of the magnetic noise, generated by the vial, filled with our ferrofluid, after it was frozen or covered by the floating plastic disk.

Fig. 3 shows the change of the spectrum of the noise generated by the vial with ferrofluid (blue) after freezing of the ferrofluid (red). It can be concluded that the freezing reduces the intensity of the magnetic noise, generated by the vial. Therefore, the vibrations of the vial with ferrofluid as a whole cannot be the main reason of the change of the magnetic flux through the SQUIDs. It can be concluded that the movement of magnetic nanoparticles relative to the walls of the vial
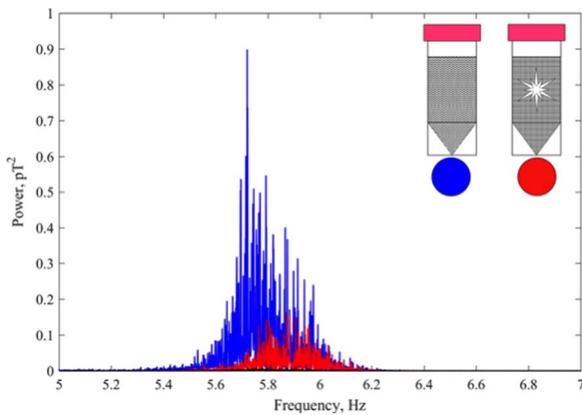
Fig. 3. The spectra of the noise generated by the vial with the ferrofluid (blue) and by the same vial after freezing of the ferrofluid (red). Black - the spectrum of the noise without the vial. The vial was located under channel 6. (For interpretation of the references to color in this figure legend, the reader is referred to the web version of this article.)
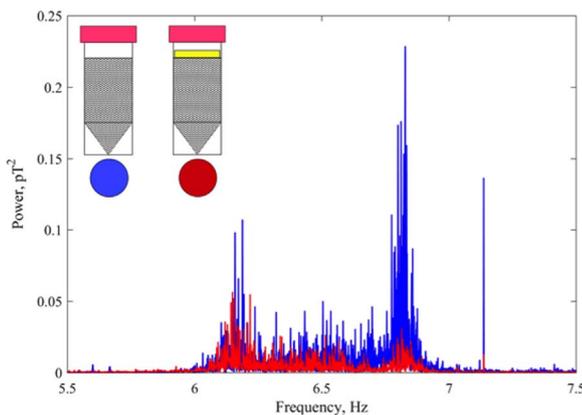
Fig. 4. The spectra of the noise generated by the vial with the ferrofluid (blue) and by the same vial after covering of the ferrofluid by the floating plastic disk (red). The vial was located under channel 6 on special platform, changing the spectrum profile. (For interpretation of the references to color in this figure legend, the reader is referred to the web version of this article.)

generates the magnetic signal.

Fig. 4 shows the change of the spectrum of the noise generated by the vial with ferrofluid (blue) after covering of the ferrofluid with the floating plastic disk (red). It can be concluded that such covering reduces the intensity of the magnetic noise, generated by the vial. This result indicates that the excitation of waves on a free surface of ferrofluid, rather than the Brownian motion of nanoparticles in its volume, is responsible for the generation of the magnetic noise.

3.3. Localization of the vial with the ferrofluid by using the acoustic noise of our experimental setup

The vial with ferrofluid was installed under the first measurement channel of the MEG device. The free surface of the ferrofluid was situated at approximately 2 centimeters below the plane of the sensors. Localization was performed in a frequency range 5.3–6.3 Hz in a cube with a side of 100 mm, which is located under the device, with a resolution of 1 mm (See 2.3).

Fig. 5 shows a functional tomogram - calculated spatial distribution of the sources of magnetic noise, generated in measuring channels of our MEG device by the vial with ferrofluid. The 3D-view of the object and its tomographic sections are shown. Also shown is the measuring device (the planar set of seven sensors) and an enlarged section through the object. The white cross indicates the position of the cursor, which is the same for all sections. The brightness of each voxel corresponds to the total power, located in this voxel. It is seen that the single bright source of the magnetic noise is located on the free surface of the ferrofluid. The noise from the volume of the ferrofluid is completely absent. So, the results of the 3D-localization of the vial with the ferrofluid in the MEG device confirm independently the conclusion about the surface nature of the magnetic noise, generated by the vial with the ferrofluid at the frequency of acoustic noise of our experimental setup.

3.4. Localization of the vial with the ferrofluid by using a human heartbeat

As was shown above, the waves on the free surface of a ferrofluid can make magnetically visible any weak mechanical oscillations. We assume that the urban environment of Moscow city was the source of detected infrasound oscillations. Infrasound is characterized by an ability to cover long distances by earth and get around obstacles with little dissipation. Therefore it can get our measurement chamber despite of special vibration-isolated foundation, shown at Fig. 1. The last fact reveals high sensitivity of the observed effect and gives hope to
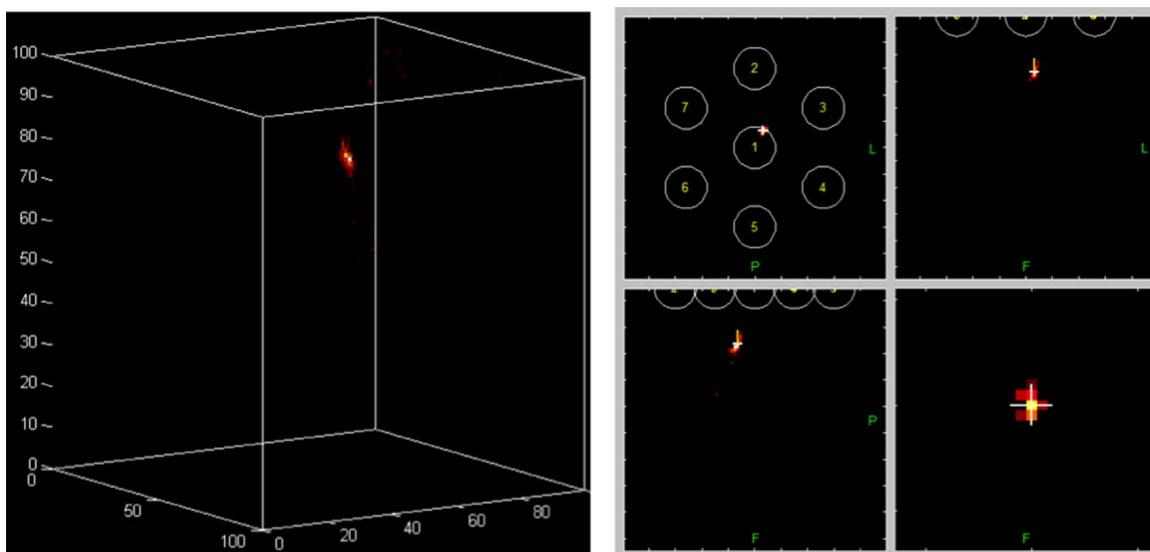
Fig. 5. 3D-view of the source of magnetic noise and its tomographic sections. Also shown is the measuring device (the planar set of seven sensors) and an enlarged section through the object. The white cross indicates the position of the cursor, which is the same for all sections. The brightness of each voxel corresponds to the total power, located at this voxel.
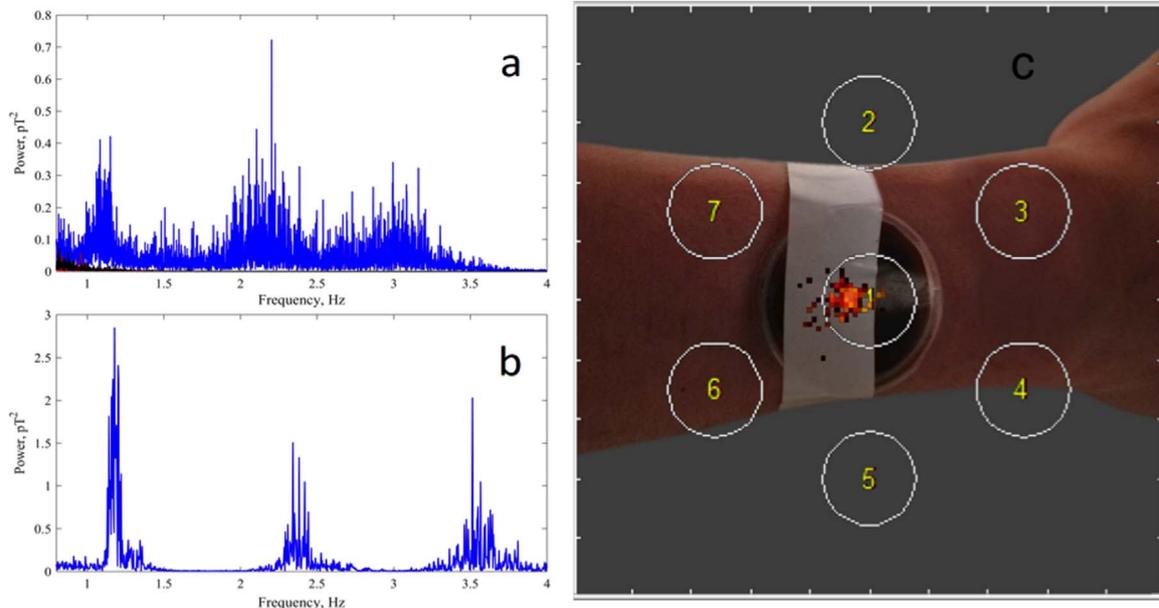
Fig. 6. a - Spectra of the ferrofluid in Petri cup, attached to the hand (blue) and of the hand without ferrofluid (black); b - Spectrum of the magnetic cardiogram, registered by the same device; c - Localization of the magnetic sources from spectral components. Spatial distribution of the spectral power of the magnetic noise sources, calculated from the spectra, is combined with hand picture. Also channels positions are shown. (For interpretation of the references to color in this figure legend, the reader is referred to the web version of this article.)

its practical use. An example of possibility to use it for contactless ballistocardiography [15] is described below.

In our demonstration experiment a Petri cap was partially filled with a ferrofluid and fixed on the hand as wristwatches. The hand was placed on the center of nonmagnetic stand situated at 8 cm under the measuring head of our 7-channel MEG device. Then MEG recordings were collected and Fourier transform of the signals from each SQUID channel was generated. In Fig. 6a such magnetically measured ballistic heartbeat spectrum is shown by a blue color. Faintly discernible background spectrum from the hand without a ferrofluid is shown on the same Fig. 6a by a black color. It is interesting to note, that measured ballistic spectrum has specific 3-peak structure, typical for magnetic cardiogram. The spectrum of the magnetic cardiogram, registered by the same 7-channel instrument in another experiment, is shown in Fig. 6b.

In Fig. 6c the spatial distribution of magnetic sources, calculated by the method [7] (see 2.3), is shown in combination with the photo of the hand. It is clear that the result of contactless magnetic localization of the heartbeat source coincides with real place of the ferrofluid fixation.

4. Conclusion

It is found, that magnetic particles imaging can be performed without pre-magnetization or displacement of the sample. The vial with ferrofluid can be localized correctly by the method [7] from multi-channel measurement of "spontaneous" magnetic fields by the 7-channel gradiometer. Quasi-random magnetic fields are generated by the particles movements produced by various sources. Registration of the tiny inherent vibrations of the instrument can be used to extra-fine tuning of the experimental setup. Amplification of the human body oscillations, such as the heartbeat, opens possible medical applications.

Acknowledgment

References

[1] B. Gleich, J. Weizenecker, Tomographic imaging using the nonlinear response of magnetic particles, Nature 435 (2005) 1214–1217.
[2] E.R. Flynn, H.C. Bryant, A biomagnetic system for in vivo cancer imaging, Phys. Med. Biol. 50 (6) (2005) 1273–1293.
[3] W. Jia, G. Xu, R.J. Sclabassi, J.G. Zhu, A. Bagic, M. Sun, Detection of magnetic nanoparticles with magnetoencephalography, J. Magn. Magn. Mater. 320 (2008) 1472–1478.
[4] T. Cheung, K. Kavanagh, U. Ribary, A new technique for magnetic nanoparticle imaging for magnetoencephalography using frequency data, Front. Neurosci. in: Conference Abstract: Biomag 2010 -Proceedings of the 17th International Conference on Biomagnetism, 2010, ⟨http://dx.doi.org/10.3389/conf.fnins06.00387⟩.
[5] Y.V. Maslennikov, The DC-SQUID-based magnetocardiographic systems for clinical use, Phys. Procedia 36 (2012) 88–93.
[6] Y.V. Maslennikov, Magnetocardiographic diagnostic complexes based on the MAG_SKAN SQUIDs, J. Commun. Technol. Electron. 56 (8) (2011) 991–999.
[7] R.R. Llinas, M.N. Ustinin, Precise Frequency-Pattern Analysis to Decompose Complex Systems into Functionally Invariant Entities: U.S. Patent, US20140107979 A1, 2014.
[8] R.R. Llinás, M.N. Ustinin, Frequency-pattern functional tomography of magnetoencephalography data allows new approach to the study of human brain organization, Front. Neural Circuits 8 (2014) 43. http://dx.doi.org/10.3389/fncir.2014.00043.
[9] R.R. Llinás, M.N. Ustinin, S.D. Rykunov, A.I. Boyko, V.V. Sychev, K.D. Walton, G.M. Rabello, J. Garcia, Reconstruction of human brain spontaneous activity based on frequency-pattern analysis of magnetoencephalography data, Front. Neurosci. 9 (2015) 373. http://dx.doi.org/10.3389/fnins.2015.00373.
[10] R.R. Llinás, M.N.Ustinin, S.Rykunov, A.I.Boyko, K.D.Walton, G.Rabello, Structure and Function of the Sources of Thalami-cortical Dysrhythmia in Human, Revealed by Magnetic Encephalography Program No. 542.13, 2015 Neuroscience Meeting Planner, Society for NeuroscienceOnline,Washington, DC, 2015.
[11] J.P. Boyd, Chebyshev and Fourier Spectral Methods, 2nd ed., NY: Dover Publishers, NewYork, 2001.
[12] M.W. Garrett, Calculation of fields, forces, and mutual inductances of current systems by elliptic integrals, J. Appl. Phys. 34 (9) (1963) 2567–2573. http://dx.doi.org/10.1063/1.1729771.
[13] R.J. Dinger, J.H.Claassen, S.A.Wolf, SQUIDS in a marine environment. in: H. Weinstock, W.C. Overton (Eds.), SQUID Applications to Geophysics, Society of Exploration Geophysicists, Tulsa, Oklahoma, 1980, p. 49, ⟨http://dx.doi.org/10.1190/1.9781560802518⟩.
[14] J. Clarke, N.E.Goldstein, Magnetotelluric measurements, in: H. Weinstock, W.C. Overton (Eds.), SQUID Applications to Geophysics, Society of Exploration Geophysicists, Tulsa, Oklahoma, 1980, p. 99, ⟨http://dx.doi.org/10.1190/1.9781560802518⟩.
[15] L. Giovangrandi, O. Inan, R. Wiard, M. Etemadi, G. Kovacs, Ballistocardiography – a method worth revisiting, Conf. Proc. IEEE Eng. Med Biol. Soc. 2011 (2011) 4279–4282. http://dx.doi.org/10.1109/IEMBS.2011.6091062.